

# Object Recognition Using Neural Networks and Complex Reflection Signals

Short paper

Hristomir Yordanov\* and Irina Topalova†

Faculty of German Engineering Education and Industrial Management  
 Technical University of Sofia, Sofia, Bulgaria  
 Emails: \*yordanov@fdiba.tu-sofia.bg, †itopalova@abv.bg

**Abstract**—Radar based imaging techniques can be used to collect 3D information about objects, which in turn can be used to identify and measure specific parameters of these objects. Such measurements need to correlate specific radar signals with the object properties. This can be done using neural networks, as they are designed to search for patterns, which are difficult to find using analytic methods. This work presents a neural network based reflection signal processing system for object identification by attempting to identify an object placed in a rectangular waveguide. We extract both the phase and the amplitude of the reflected signal and compare recognition systems using amplitude only and using both phase and amplitude.

**Keywords**—Scattering signals; Object identification; Neural Networks

## I. INTRODUCTION

Radars find many applications as imaging tools. Using the property of electromagnetic waves to partially penetrate and partially reflect from dielectric materials, they can provide 3D images of a large set of objects. The development of easily available high-frequency components up in the microwave, millimeter wave and even terahertz ranges allows for high spatial resolution of the obtained images. This technique finds multiple applications in security systems, in medical systems and in agriculture.

We can consider as an example the sensor described in [2]. The system consists of a 24 GHz Frequency Modulated Continuous Wave (FMCW) radar used to make 3D images of grapevine plants in order to estimate the volume of grapes in a given plant. The radar is equipped with a high gain antenna and is mounted on a pan-tilt platform, which allows for performing azimuthal and elevation scans. The radar bandwidth is 2 GHz. This setup allows for a 7.5 cm depth resolution (that is the precision of the measurement of the distance between the object and the radar) and transverse resolution of 1.5 cm. Of course, using higher signal frequency, bandwidth and more directive antennas, resolutions in the millimeter range can be achieved [3].

The processing of the radar signal in order to obtain information about the object parameters of interest can be a challenging task. The measurement system described in [2] relies on statistical analysis in order to obtain the grapes volume. Neural networks are optimized for pattern search in complex data. Therefore, they can be used in radar based measurement systems as they can extract the data of interest from the clutter and simultaneously estimate the value of the

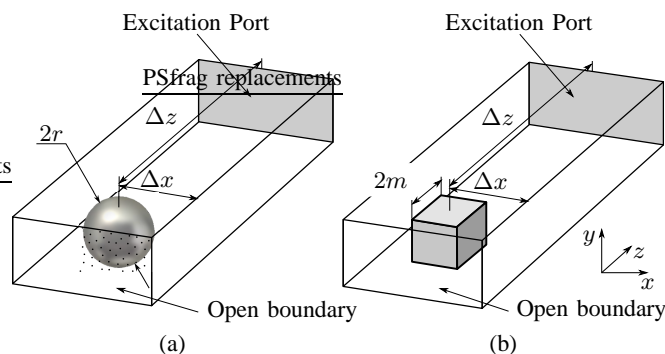


Fig. 1. Positioning of a ball of a diameter  $2r$  (a) and a cube with edge  $2m$  (b) in a WG-12 rectangular waveguide.

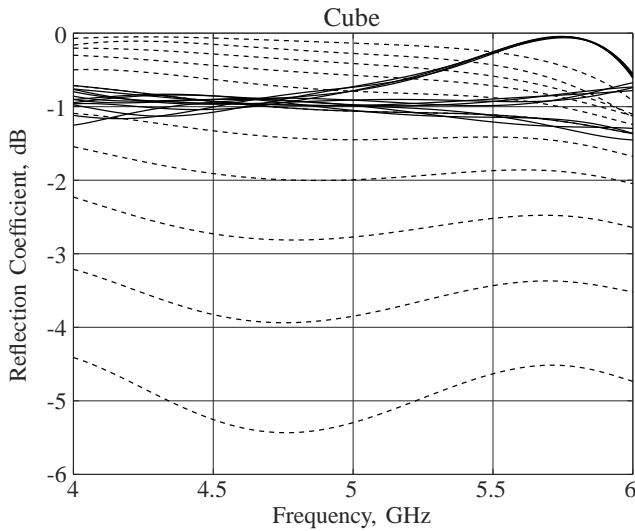
parameter of interest. In the grapevines radar example, the parameter of interest is the volume of the produced grapes and the clutter is the signals from the plant's trunk and leaves.

In order to develop an intelligent 3D image processing system, we need to start by implementing simple 1D solutions. In this paper, we present a neural network for shape recognition based on the scattered signal as a benchmark case study. The investigated object is a body of perfectly conducting material placed in a rectangular hollow waveguide. This limits the neural network input signal to the spectral representation of a single point reflection signal. We have previously presented identifying simple objects using just the amplitude of the reflected signal [1]. In this paper we consider both the amplitude and the phase of the scattered wave. The setup has been modeled numerically and the scattering parameters have been obtained using computer simulation.

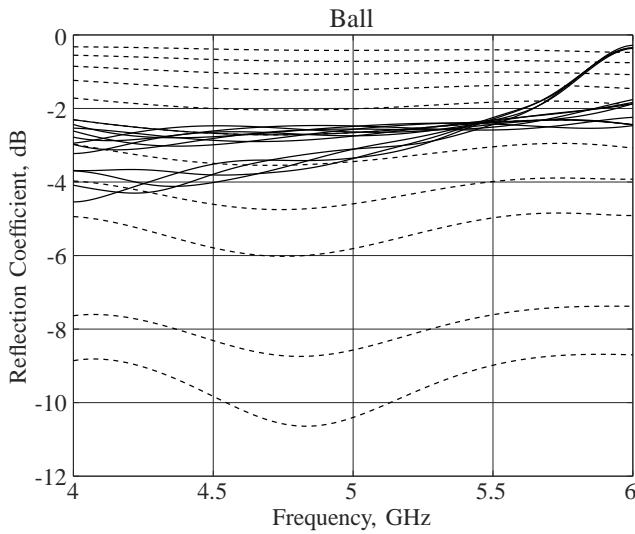
Section II describes the setup of the performed simulation and shows the computed reflected signals from the two types of objects in a waveguide. Section III details the neural network based signal processing used to identify the objects based on the reflected signal. Section II discusses the obtained experimental results and Section V summarizes the paper and sketches the future work.

## II. EXPERIMENTAL SETUP

The experimental setup consists of a hollow rectangular WG12 waveguide with an object placed at distance  $\Delta z$  from the excitation port, as shown in Figure 1. The cross-sectional dimensions of the waveguide are  $a = 47.5$  mm



(a)

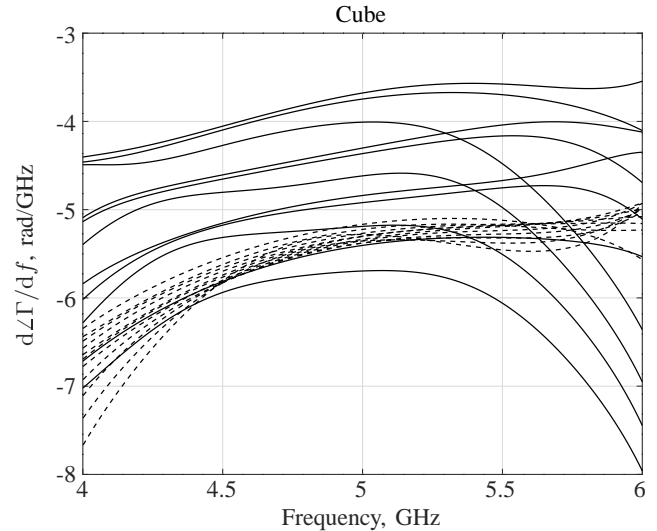


(b)

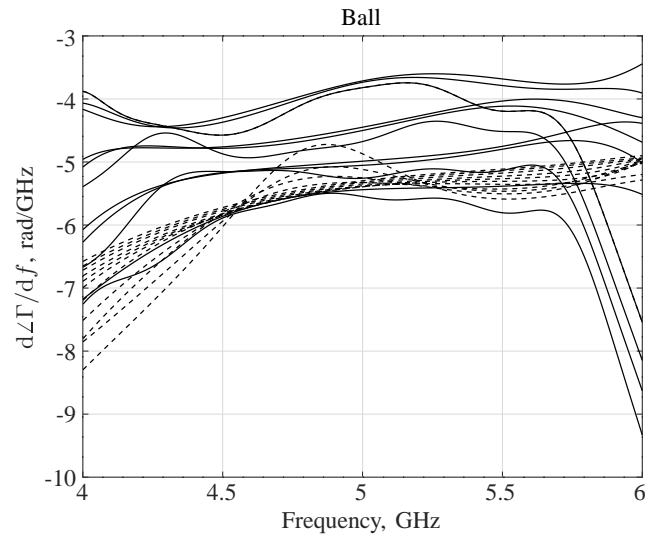
Fig. 2. Family of curves showing the magnitude of the reflection coefficient of a waveguide with a conducting cube (a) and a sphere (b) inside. The solid lines and the dotted lines represent varying position and size of the sphere respectively.

and  $b = 22.1$  mm. The scattering objects are a sphere of radius  $r$  (Figure 1a) and a cube of length  $2m$  (Figure 1b). Both objects are made of a perfect electric conductor and are placed at a distance  $\Delta x$  from the short wall of the conductor. The objects were placed in the middle of the waveguide in the vertical  $y$  direction. The excitation port has been placed at the  $-z$  end of the waveguide. The opposite end has been terminated with an open boundary in order to model an infinitely extended waveguide and thus eliminate the reflections from that boundary. The model has been simulated for the frequency range of 4 to 6 GHz, which corresponds to the full single mode range of the waveguide. We measure the reflection coefficient at the excitation port. The used simulation tool is CST Microwave studio.

Two families of results have been generated. First, we varied the dimensions of the objects—the sphere radius  $r$  and the



(a)



(b)

Fig. 3. Family of curves showing the derivative of the phase with respect to frequency of the reflection coefficient of a waveguide with a conducting cube (a) and a sphere (b) inside. The solid lines and the dotted lines represent varying position and size of the sphere respectively.

cube edge  $2m$  respectively—while keeping both objects at fixed position  $\Delta z = 100$  mm and  $\Delta x = a/2$ , that is 100 mm from the excitation port and in the middle along the  $x$  direction. The size parameters  $r$  and  $m$  varied from 4 to 10 mm in 0.6 mm steps. Then, we held the object dimensions fixed at  $r, m = 7$  mm and varied the offset dimension as follows:

$$\Delta z = 0 \text{ to } -30 \text{ mm in } 10 \text{ mm steps,}$$

$$\Delta x = 0 \text{ to } 10 \text{ mm in } 5 \text{ mm steps.}$$

The full combination of offset coefficients has been modeled.

We consider both the amplitude and the phase of the reflected signal, relative to the incident one. This is defined as the complex reflection coefficient  $\Gamma$  of the perturbed waveguide [4]. The amplitude and the phase are two independent variables and we can get more information about the shape of the object in the waveguide if we consider both of them instead

of just one. The information carried by the distribution of the amplitude of the reflection coefficient in frequency  $\Gamma(f)$  can be extracted straightforward by feeding it directly to a neural network, as we proceed in Section III. There is an intrinsic difficulty in working with the phase, though, because we can not distinguish a  $2\pi$  phase increment:  $\angle\Gamma = \angle\Gamma \pm n2\pi$ . In other words, the reflection coefficient generated by a perfectly conducting transverse wall, shorting a lossless waveguide, will be the same as the one when the wall is moved  $\pm\lambda_g/2$  in longitudinal direction, where  $\lambda_g$  is the length of the guided wave. This can cause significant difficulties for an intelligent system, trying to identify the shape of the object irrespective of the distance of interrogation.

We attempt to circumvent this problem by using the derivative of the phase of the reflection coefficient with respect to the frequency  $d\angle\Gamma/df$ , measured in rad/Hz, instead of the phase itself. In this way we disregard any  $\pm n2\pi$  uncertainty while keeping the information about the distribution of the phase in frequency.

The results for the amplitude of the reflection coefficient for a cube and a ball are presented in Figures 2a and 2b, respectively, where the dotted lines show the family of curves for varying object size, while the position is held fixed, and the solid lines show the results for fixed size and varying offset. The dotted lines show a greater reflection coefficient as the object dimensions  $r$  and  $m$  increase, which can be expected as larger objects create larger echo. The derivative of the phase with respect to frequency for a cube and a ball is presented in Figures 3a and 3b respectively.

We have used a combination of the frequency distribution of the magnitude and phase of the reflection coefficient in order to generate an input for the shape recognition neural network. We have used 11 points from each of the curves from Figures 2 and 3, as the frequency response varies slowly and using this representation we lose no information. Thus we get an input signal of 22 points for each size and position of the respective object. As the number of size and position varying simulations is also 22, we get 22 input signals of 22 points each for each object. We use 14 of those signals to train the network and 8 to test it.

We compare the efficiency of a shape recognizing neural network working with reflection coefficient amplitude and phase versus a system working with amplitude only. We use 11 points from each amplitude curve, presented in Figure 2 in order to train and test such a network.

### III. NEURAL NETWORK SIGNAL PROCESSING

There are various studies concerning the pre-processing of input data for the recognition system to improve its efficiency and accuracy. In order to make a correct choice of the recognition method, it is necessary to analyze the data defining the parametric descriptions of the objects. This analysis is based on the calculation of the statistical parameters of the data as well as the determination of the degree of similarity between the parametric descriptions of the objects. Since our study involves highly correlated input parametric vectors representing parametric descriptions of the reflected radar signal for the

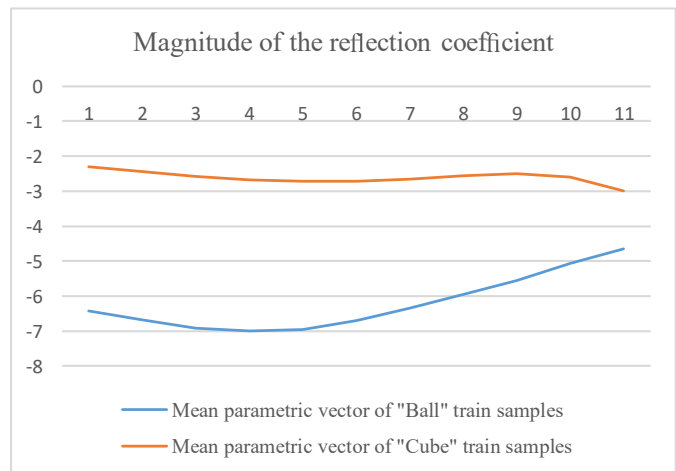


Fig. 4. Mean parametric vectors over the magnitudes of the reflection coefficients for 14 train samples of “ball” and “cube”.

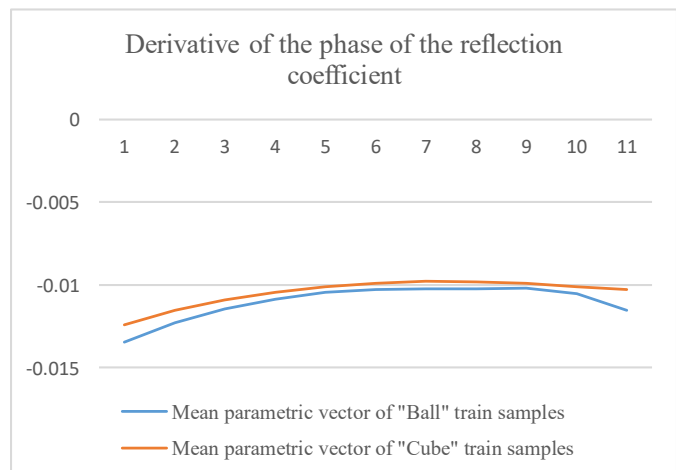


Fig. 5. Mean parametric vectors over the derivative of the phase of the reflection coefficients for 14 train samples of “ball” and “cube”.

two objects under study, we have chosen the adaptive neural network method, that provides the most effective recognition of similar input data. As the two 3D objects have similar shapes, it is necessary to use an adaptive and precise method for recognition and classification of the two objects. The Deep Learning method using a Multi-Layered-Perception (MLP) feed forward Neural Network (NN), trained by the Back-propagation (BP) algorithm, gives satisfactory results in the cases described in [5], [6]. This allows precise placement of boundaries between object classes with overlapping parametric descriptions – in our case very similar reflection signals. In order for the neural network to be “assisted” in advance, different linear transformations (mostly scaling to the ranges of  $(0, 1)$  or  $(-1, 1)$ ) [7], [8], statistical standardization (using deviation from the mean) or various other appropriate mathematical transformations over the input data [9], [10] are suggested. In our study, in order to reduce the preliminary calculations and simplify the method, we choose an appropriate combination of independent parameters of the reflected radar signal, such as magnitude and phase of the reflection coefficient.

TABLE I. STANDARD DEVIATION AND CORRELATION BETWEEN THE MEAN PARAMETRIC VECTORS

Input data	Standard deviation		Correlation between mean parametric vectors
	Ball	Cube	
$ \Gamma $	0.801	0.179	-0.337
$d\Delta\Gamma/df$	$1.05 \cdot 10^{-3}$	$8.29 \cdot 10^{-4}$	0.972
$\Gamma$	3.217	1.337	0.976

### A. Preprocessing stage

In this stage some statistical parameters of the signals are calculated, in order to evaluate the correlation between the signals representing the two objects and the mean square deviation of the signal parameters concerning the training samples for each of the two objects. For this purpose, the mean parametric vectors of the magnitude, of the derivative of the phase of the reflection coefficient and of the complex signal (combining both of them) are calculated. The obtained mean parametric vectors for 14 train samples of “ball” and “cube” are shown in Figures 4 and 5, respectively.

The next step is to evaluate the standard deviation for each of these two signals and calculate the correlation between the mean parametric vectors of “ball” and “cube”. Considering these two parameters, it is easier to make decision what kind of a recognition method to apply, since with a high correlation of interclass parametric descriptions, it is recommended to choose an adaptive recognition method, such as a neural network.

On the other hand, the adaptation of the neural network and, respectively, the accuracy of recognition in this case would be much more efficient, if the standard mean square deviation of the input training parameter vectors within the class is higher. The correlation between the mean parametric vectors over the magnitudes, the derivative of the phase of the reflection coefficients and over the complex (magnitude and derivative of the phase) signal for 14 training samples of “ball” and “cube” respectively, is has been calculated using the Pearson correlation coefficient [11]:

$$\rho_{\text{ball,cube}} = \frac{\sum_{i=1}^n (B_i - \bar{B})(C_i - \bar{C})}{\sqrt{\sum_{i=1}^n (B_i - \bar{B})^2 (C_i - \bar{C})^2}}, \quad (1)$$

where  $B_i$ ,  $C_i$  is the current component of the input vector “cube/ball”, and  $n$  is the number of components ( $n = 11$  for input vector “magnitude” and “derivative of the phase”;  $n = 22$  for the “complex” vector). The achieved results for the discussed calculated parameters are shown in Table I, where  $\Gamma$  is the complex reflected signal,  $|\Gamma|$  is its magnitude, and  $d\Delta\Gamma/df$  is the derivative if the phase of the reflection signal with respect to the frequency. The obtained results show that the correlation has the lowest values for input data “magnitude”, but the standard deviation is highest at the complex signal. Thus we will train a MLP neural network (MLP NN) with “magnitude” and “complex” signals, aiming to compare the recognition accuracy results.

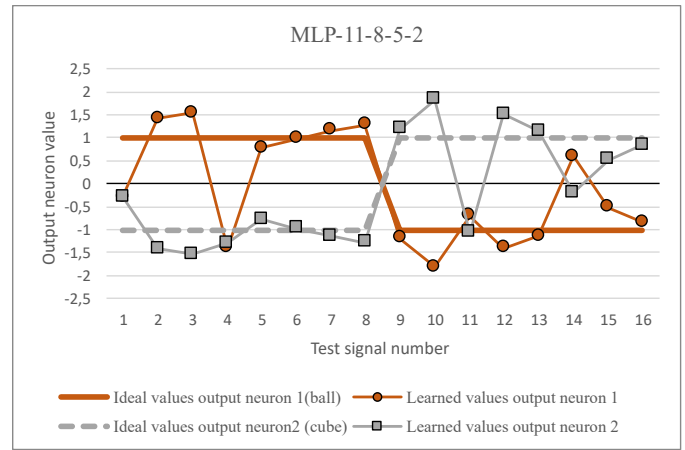


Fig. 6. MLP NN (11-8-5-2) output results for Output neuron 1 (ball) and for Output neuron 2 (cube) when recognizing the 8 exemplars of objects ball and cube with “magnitude” input vector

### B. Neural network: structure and training method

We have trained the MLP NN in two cases: first only with “magnitude” input signal, sampling 11 points from each curve, as they vary slowly in frequency and second with “complex” signal having 22 points respectively. In both cases the training set contains 14 curves with varying offset and object size. The test set contains 8 specimens, representing the two types of objects, whose reflected signals have not participated in the training set. For the first case we have designed the MLP NN by adding two hidden layers and increasing the number of neurons in each layer until satisfactory recognition was achieved. The best recognition results were obtained in the case MLP 11-8-5-2 structure (with two hidden layers, having 8 and 5 neurons and 2 output neurons, representing the two recognizable objects), with a reached minimum Mean Square Error (MSE- $\epsilon$ ) of 5%. For the second case we train different MLP structures of 22-10-2; 22-15-2 and 22-20-2 neurons with a reached a few times less minimum MSE- $\epsilon$ ) of 0.02 and 0.04%.

In both cases a step by step “continue” stage of the training has been applied, reducing the error achieved and accepted at each previous stage. We use steps obtaining MSE of 5%; 1%; 0.8%; 0.4%; 0.1%; 0.08%; 0.04%; 0.02%. This method permits fine tuning (FT) of a pre-trained network using slightly changed training data.

## IV. EXPERIMENTAL RESULTS

The MLP NN output results when recognizing the 8 specimens, representing the two objects, whose reflected signals have not participated in the training set, are shown in Figures 6 to 10. Figure 6 represents the NN outputs 1 and 2, when training the network only with “magnitude” input data for a 11-8-5-2 MLP NN. In this case the obtained recognition accuracy is 75% for both objects, that is, 2 samples of each object are falsely recognized. The training iterations were stopped when the MSE has reached 5%. Figures 7, 8 and 9 show the NN outputs 1 and 2, when training the network with “complex” input data, respectively with different MLP NN structures: 22-10-2; 22-15-2 and 22-20-2. In order to put

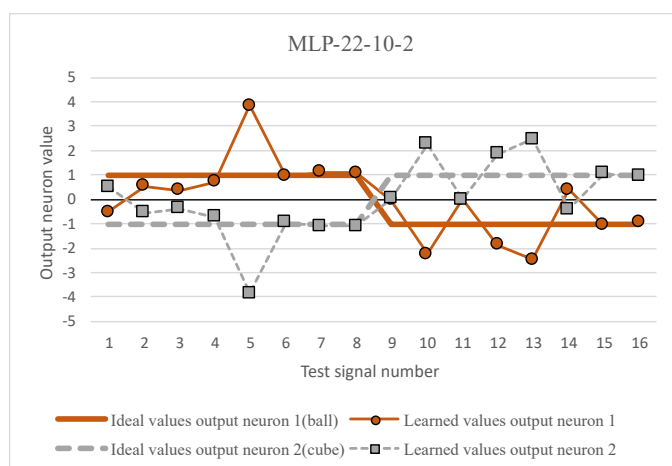


Fig. 7. MLP NN (22-10-2) output results for Output neuron 1 (ball) and for Output neuron 2 (cube) when recognizing the 8 exemplars of objects ball and cube with “complex” input vector

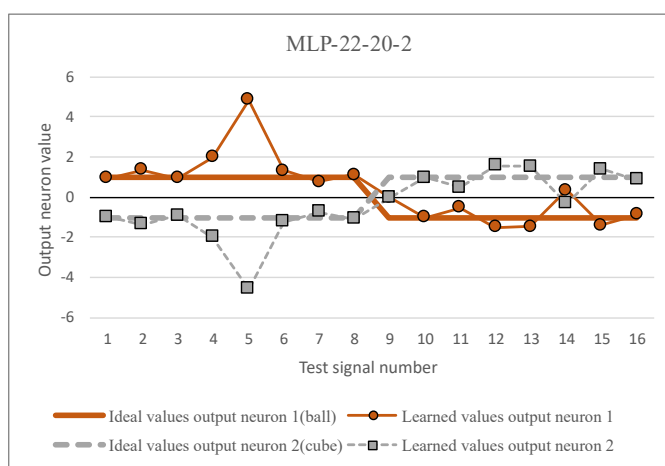


Fig. 9. MLP NN (22-20-2) output results for Output neuron 1 (ball) and for Output neuron 2 (cube) when recognizing the 8 exemplars of objects ball and cube with “complex” input vector

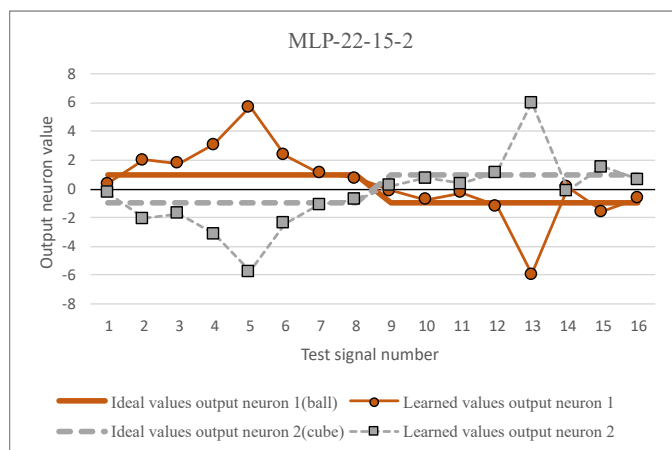


Fig. 8. MLP NN (22-15-2) output results for Output neuron 1 (ball) and for Output neuron 2 (cube) when recognizing the 8 exemplars of objects ball and cube with “complex” input vector

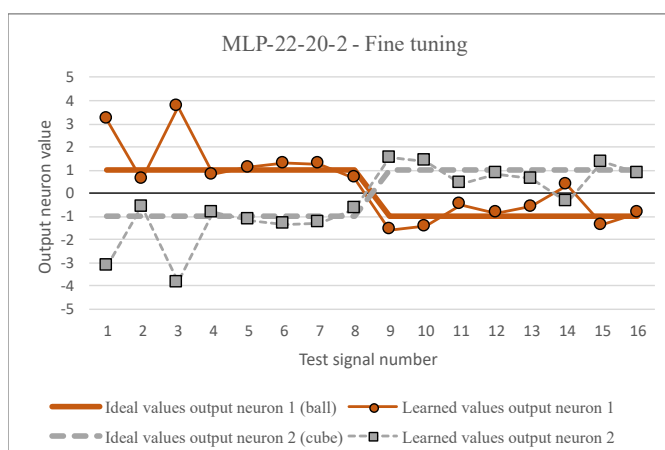


Fig. 10. MLP NN (22-20-2) output results for Output neuron 1 (ball) and for Output neuron 2 (cube) when recognizing the 8 exemplars of objects ball and cube with “complex” input vector applying fine tuning training

more precise boundaries between the object classes and to improve the accuracy of recognition, it is necessary to increase the number of neurons in the hidden layer of the MLP NN. Thus, each subsequent train and test step is made with an increased number of neurons in the hidden layer. It is good recognizable that the approximation of ideal/ learned values is improved after each subsequent increase of neurons in the hidden layer. For object “ball” the accuracy increases from 87.5% to 100% and for “cube” – from 62.5% (3 samples out of 8 are misidentified) to 87.5% (1 sample out of 8 is misidentified). Figure 10 represents the NN outputs in test phase, when fine tuning train method was applied. The obtained approximation error for the various structures is shown in Figure 11. Obviously, the best approximation was achieved in the case of MLP 22-20-2 and fine tuning training. The summary of the achieved recognition accuracy and the reached MSE for all tested cases, is shown in Table II.

### V. CONCLUSION

This paper shows the initial work on identifying suitable neural network signal processing tools for radar based shape

recognition techniques. The achieved recognition results show that it is very appropriate to implement MLP NN for 3D object recognition, when using radar reflection signals. The good approximation abilities of the MLP NNs make it possible to recognize even objects of very similar shapes. It has been shown that a complex signal that has a higher value for standard deviation, results in effective training and therefore in better recognition accuracy. As future work, we intend to test the method for a larger number of objects with similar 3D

TABLE II. RECOGNITION ACCURACY FOR DIFFERENT MLP STRUCTURES AND INPUT SIGNALS

Input Data	MLP structure	Recognition Accuracy, %		
		Ball	Cube	MSE-ε
Magnitude	11-8-5-2	75%	75%	5%
Complex	22-10-2	87.5%	62.5%	0.02%
Complex	22-15-2	100%	75%	0.02%
Complex	22-20-2	100%	87.5%	0.04%

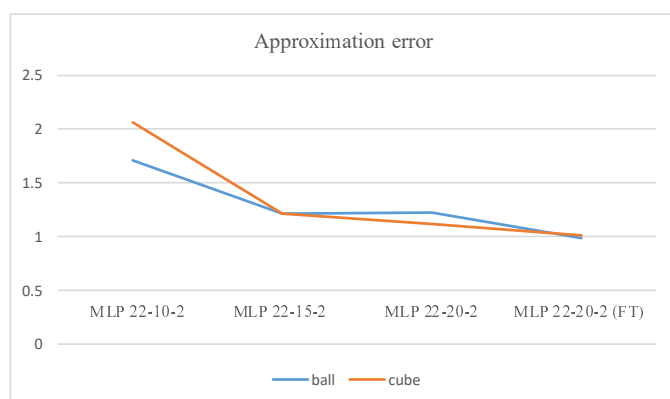


Fig. 11. Achieved approximation error for "complex" input vector with different MLP NN structures.

object shapes. Also, to generalize the method, the test sample set will be increased. Additional calculations of approximation error are also foreseen. The presented results provide shape recognition by a single point wideband reflected signal, which is a model of a pulse radar. We intend to expand these results toward scanning pulsed and scanning frequency modulated continuous wave (FMCW) radars.

#### REFERENCES

- [1] H. Yordanov and I. Topalova, "Neural networks for scattering signal based object recognition," in *The Fourteenth International Conference on Autonomic and Autonomous Systems ICAS 2018*, May 2018, pp. 1–3.
- [2] D. Henry, H. Aubert, T. Veronese, and E. Serrano, "Remote estimation of intra-parcel grape quantity from three-dimensional imagery technique using ground-based microwave FMCW radar," *IEEE Instrumentation Measurement Magazine*, vol. 20, no. 3, pp. 20–24, June 2017.
- [3] K. B. Cooper, R. J. Dengler, N. Lombart, T. Bryllert, G. Chattopadhyay, E. Schlecht, J. Gill, C. Lee, A. Skalare, I. Mehdi, and P. H. Siegel, "Penetrating 3-d imaging at 4- and 25-m range using a submillimeter-wave radar," *IEEE Transactions on Microwave Theory and Techniques*, vol. 56, no. 12, pp. 2771–2778, Dec 2008.
- [4] D. M. Pozar, *Microwave Engineering*, 3rd ed. Ney York, NY: John Wiley & Sons, 2005.
- [5] J. Schmidhuber, "Deep learning in neural networks: An overview," *Neural Networks*, vol. 61, pp. 85–117, 2015. [Online]. Available: <http://www.sciencedirect.com/science/article/pii/S0893608014002135>
- [6] *NeuroSystems V4.0 Manuall*. Germany: Siemens GmbH, 2016.
- [7] N. M. Nawi, W. H. Atomi, and M. Rehman, "The effect of data pre-processing on optimized training of artificial neural networks," *Procedia Technology*, vol. 11, pp. 32–39, 2013, 4th International Conference on Electrical Engineering and Informatics, ICEEI 2013. [Online]. Available: <http://www.sciencedirect.com/science/article/pii/S2212017313003137>
- [8] K. Kuźniar and M. Zajac, "Some methods of pre-processing input data for neural networks," *Computer Assisted Methods in Engineering and Science*, vol. 22, no. 2, pp. 141–151, 2017. [Online]. Available: <http://comes.ippt.gov.pl/index.php/comes/article/view/33>
- [9] I. Topalova and M. Uzunova, "Recognition of similar marble textures through different neural networks with de-correlated input data," *International Journal on Advances in Intelligent Systems*, vol. 10, pp. 474–479, 2017. [Online]. Available: [http://www.iariajournals.org/intelligent\\_systems/](http://www.iariajournals.org/intelligent_systems/)
- [10] I. Topalova, "Automated marble plate classification system based on different neural network input training sets and plc implementation," *International Journal of Advanced Research in Artificial Intelligence*, vol. 1, no. 2, pp. 50–56, 2012. [Online]. Available: <http://dx.doi.org/10.14569/IJARAI.2012.010209>
- [11] J. L. Rodgers and W. A. Nicewander, "Thirteen ways to look at the correlation coefficient," *The American Statistician*, vol. 42, no. 1, pp. 59–66, 1988. [Online]. Available: <https://doi.org/10.1080/00031305.1988.10475524>